Inorganic Chemistry
Article

Mixed-Ligand Copper(II)-phenolate Complexes: Effect of Coligand on Enhanced DNA and Protein Binding, DNA Cleavage, and Anticancer Activity

Venugopal Rajendiran,[†] Ramasamy Karthik,[†] Mallayan Palaniandavar,*,[†] Helen Stoeckli-Evans,[‡] Vaiyapuri Subbarayan Periasamy,[§] Mohammad Abdulkader Akbarsha,[§] Bangalore Suresh Srinag,[∥] and Hanumanthappa Krishnamurthy[∥]

School of Chemistry, Bharathidasan University, Tiruchirapalli 620 024, India, Institut de Chimie, Université de Neuchâtel, Avenue de Bellevaux 51, C.P.2, CH-2007 Neuchâtel, Switzerland, Department of Animal Science, Bharathidasan University, Tiruchirapalli 620 024, India, National Centre for Biological Science, Tata Institute for Fundamental Research, Bangalore 560 065, India

Received April 20, 2007

The copper(II) complex [Cu(tdp)(ClO₄)]·0.5H₂O (**1**), where H(tdp) is the tetradentate ligand 2-[(2-(2-hydroxyethylamino)-ethylimino)methyl]phenol, and the mixed ligand complexes [Cu(tdp)(diimine)]⁺ (**2**–**5**), where diimine is 2,2′-bipyridine (bpy) (**2**), 1,10-phenanthroline (phen) (**3**), 3,4,7,8-tetramethyl-1,10-phenanthroline (tmp) (**4**), and dipyrido-[3,2-*d*: 2′,3′-*f*]-quinoxaline (dpq) (**5**), have been isolated and characterized by analytical and spectral methods. Complexes **1** and [Cu(tdp)(phen)]ClO₄ (**3**) have been structurally characterized, and their coordination geometries around copper-(II) are described as distorted octahedral. The equatorially coordinated ethanolic oxygen in **1** is displaced to an axial position upon incorporating the strongly chelating phen, as in **3**. The solution structures of all the complexes have been assessed to be square-based using electronic absorption and electron paramagnetic resonance (EPR) spectroscopy. The interaction of the complexes with calf thymus DNA (CT DNA) has been explored by using absorption, emission, and circular dichroic spectral and viscometric studies, and modes of DNA binding for the complexes have been proposed. Absorption spectral (K_b = 0.071 ± 0.005 (**2**), 0.90 ± 0.03 (**3**), 7.0 ± 0.2 (**4**), 9.0 ± 0.1 × 10⁵ M⁻¹ (**5**)), emission spectral (K_{app} = 4.6 (**1**), 7.8 (**2**), 10.0 (**3**), 12.5 (**4**), 25.0 × 10⁵ M⁻¹ (**5**)), and viscosity measurements reveal that **5** interacts with DNA more strongly than the other complexes through partial intercalation of the extended planar ring of the coordinated dpq with the DNA base stack. Interestingly, only complex **4** causes a B to A conformational change upon binding DNA. All the complexes hydrolytically cleave pBR322 supercoiled DNA in 10% DMF/5 mM Tris-HCl/50 mM NaCl buffer at pH 7.1 in the absence of an activating agent, and the cleavage efficiency varies in the order **5** > **3** > **2** > **4** > **1** with **5** displaying the highest K_{cat} value (5.47 ± 0.10 h⁻¹). The same order of cleavage is observed for the oxidative cleavage of DNA in the presence of ascorbic acid as a reducing agent. Interestingly, of all the complexes, only **5** displays efficient photonuclease activity through double-strand DNA breaks upon irradiation with 365 nm light through a mechanistic pathway involving hydroxyl radicals. The protein binding ability of **1**–**5** has been also monitored by using the plasma protein bovine serum albumin (BSA), and **4** exhibits a protein binding higher than that of the other complexes. Further, the anticancer activity of the complexes on human cervical epidermoid carcinoma cell line (ME180) has been examined. Interestingly, the observed IC₅₀ values reveal that complex **4**, which effects conformational change on DNA and binds to BSA more strongly, exhibits a cytotoxicity higher than the other complexes. It also exhibits approximately 100 and 6 times more potency than cisplatin and mitomycin C for 24 and 48 h incubation times, respectively, suggesting that **4** can be explored further as a potential anticancer drug. Complexes **4** and **5** mediate the arrest of S and G₂/M phases in the cell cycle progression at 24 h harvesting time, which progress into apoptosis.

Introduction

One of the most rapidly developing areas of pharmaceutical research is discovery of drugs for cancer therapy.

Cisplatin [*cis*-diamminedichlorideplatinum(II)] is one of the foremost and widely used metal-based anticancer drug.[1,2] Lippard and co-workers have elucidated the detailed molecular mechanism of its action, which involves its covalent binding to DNA.[3] Although the drug is one of the most active anticancer drugs and is curative in some tumor types,[4] its

---

* To whom correspondence should be addressed. E-mail: palanim51@yahoo.com.
† School of Chemistry, Bharathidasan University.
‡ Insitute de Chimie, Université de Neuchâtel.
§ Department of Animal Science, Bharathidasan University.
∥ National Centre for Biological Science, Tata Institute for Fundamental Research.

(1) Boulikas, T.; Vougiouka, M. *Oncol. Rep.* **2003**, *10*, 1663−1682.
(2) Wong, E.; Giandomenico, C. M. *Chem. Rev.* **1999**, *99*, 2451−2466.
(3) Jamieson, E. R.; Lippard, S. J. *Chem. Rev.* **1999**, *99*, 2467−2498.

use is limited[5,6] by both its side-effects and acquired cellular resistance. So more-efficacious, less toxic, and target-specific noncovalently DNA binding anticancer drugs are to be developed. Generally anticancer agents that are approved for clinical use are molecules which damage DNA, block DNA synthesis indirectly through inhibition of nucleic acid precursor biosynthesis, or disrupt hormonal stimulation of cell growth.[7] Therefore, considerable effort has been now focused on the developement of new anticancer drugs based on transition metal complexes, particularly, biocompatible copper(II) complexes, that bind to and cleave DNA[8] under physiological conditions. Also these complexes must recognize nucleic acids, particularly, in a sequence-specific fashion and then bind to them in a way that alters their function. Copper complexes, which possess biologically accessible redox potentials and demonstrate high nucleobase affinity, are potential reagents for cleavage of DNA both oxidatively[9] and hydrolytically.[8] The ability of copper complexes to cleave DNA upon photoactivation under physiological conditions have also received considerable attention[10,11] because of their possible utility in highly targeted photodynamic therapeutic applications.[12]

Copper(II) complexes of 1,10-phenanthroline (phen) ligands, which cleave DNA duplexes,[13−16] show antiviral activity upon interaction with nucleic acid templates and inhibit proviral DNA synthesis.[13] Very recently, Reedijk and co-workers have reported that the complex [Cu^{II}(pyrimol)Cl], where Hpyrimol is 4-methyl-2-[(pyrid-2-ylmethylene)amino]-phenol, shows efficient self-activated DNA cleavage and
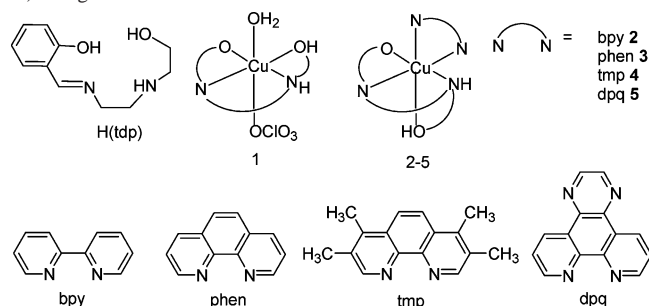
cytotoxic effects on L1210 murine leukemia and A2780 human ovarian carcinoma cell lines.[17] Recently, there has been substantial interest in the design and study of DNA binding[18] and cleavage properties of mixed-ligand Cu(II) complexes[19] and development of the complexes as metallodrugs. Sadler and his co-workers have reported mixed ligand bis(salicylato)copper(II) complexes with diimines as coligands to exhibit cytotoxic and antiviral activities.[20] Guo and his co-workers have reported the ternary Cu(II) complex of 1,10-phenanthroline and L-threonine, which hydrolytically cleave DNA and exhibit cytotoxicity.[21] Like DNA, proteins are also now considered[22] to be one of the main molecular targets in the action of anticancer agents.[23] The significance of these drug targets is clearly shown by the high incidence of alterations in the genes that code for the proteins in tumors, and attention has been now focused on the proteins that drive and control cell cycle progression.[22]

The present work stems from our continuous interest in defining and evaluating the key DNA and protein binding and DNA cleavage of copper(II) complexes of diimine ligands[18,24] and also from our efforts to explore the structure−activity relationship for the cleavage. In this article, we isolated the copper(II) complex [Cu(tdp)(ClO$_4$)]·0.5H$_2$O (**1**), where H(tdp) is the tetradentate ligand 2-[(2-(2-hydroxyethylamino)ethylimino)methyl]phenol, and a series of mixed-ligand copper(II) complexes of the type [Cu(tdp)(diimine)]-(ClO$_4$), where diimine = 2,2′-bipyridine (bpy) (**2**), 1,10-phenanthroline (phen) (**3**), 3,4,7,8-tetramethyl-1,10-phenanthroline (tmp) (**4**), or dipyrido-[3,2-*d*:2′;3′-*f*]-quinoxaline (dpq) (**5**) (Scheme 1) and explored their ability to bind to protein and DNA and also to cleave DNA. The tetradentate phenolate ligand is designed to provide donor elements such as amine, phenolate, and ethanolic groups and thus tune the DNA- and protein-binding and DNA-cleaving properties of the complexes. On the other hand, phen and other diimines are used for recognizing and binding to DNA, and thus the methyl groups on the 3,4,7,8-positions of the phen ring, like

(4) Galanski, M.; Arion, V. B.; Jakupec, M. A.; Keppler, B. K. *Curr. Pharm. Des.* **2003**, *9*, 2078−2089.

(5) Tanaka, T.; Yukawa, K.; Umesaki, N. *Oncol. Rep.* **2005**, *14*, 1365−1369.

(6) (a) Wang, D.; Lippard, S. J. *Nat. Rev. Drug Discovery* **2005**, *4*, 307−320. (b) Berners- Price, S. J.; Appleton, T. G. In *Platinum-Based Drugs in Cancer Therapy*; Kelland, L. R., Farrell, N., Eds.; Humana Press: Totowa, NJ, 2000; pp 3−31. (c) Angeles-Boza, A. M.; Bradley, P. M.; Fu, P. K.-L.; Wicke, S. E.; Bacsa, J.; Dunbar, K. M.; Turro, C. *Inorg. Chem.* **2004**, *43*, 8510−8519.

(7) Foye, W. O. *Cancer Chemotherapeutic Agents*; American Chemical Society: Washington, DC, 1995.

(8) (a) Hegg, E. L.; Burstyn, J. N. *Coord. Chem. Rev.* **1998**, *173*, 133−165. (b) Mancin, F.; Scrimin, P.; Tecilla, P.; Tonellato, U. *Chem. Commun.* **2005**, 2540−2548. (c) An, Y.; Liu, S. -D.; Deng, S. -Y.; Ji, L. -N.; Mao, Z. -W. *J. Inorg. Biochem.* **2006**, *100*, 1586−1593.

(9) (a) Sigman, D. S.; Bruce, T. W.; Sutton, C. L. *Acc. Chem. Res.* **1993**, *26*, 98−104. (b) Sigman, D. S. *Acc. Chem. Res.* **1986**, *19*, 180−186. (c) Pogozelski, W. K.; Tullius, T. D. *Chem. Rev.* **1998**, *98*, 1089−1107.

(10) (a) Boerner, L. JK.; Zaleski, J. M. *Curr. Opin. Chem. Biol.* **2005**, *9*, 135−144. (b) Armitage, B. *Chem. Rev.* **1998**, *98*, 1171−1200.

(11) (a) Dhar, S.; Senapati, D.; Das, P. K.; Chattopaddhyay, P.; Nethaji M.; Chakravarty, A. R. *J. Am. Chem. Soc.* **2003**, *125*, 12118−12124. (b) Patra, A. K.; Dhar, S.; Nethaji M.; Chakravarty, A. R. *Chem. Commun.* **2003**, 1562−1563. (c) Dhar, S.; Senapati, D.; Reddy, P. A. N.; Das, P. K.; Chakravarty, A. R. *Chem. Commun.* **2003**, 2452−2453.

(12) (a) Bradley, P. M.; Angeles-Boza, A. M.; Fu, P. K. -L.; Dunbar, K. R.; Turro, C. *Inorg. Chem.* **2004**, *43*, 2450−2452. (b) Angeles-Boza, A. M.; Bradley, P. M.; Fu, P. K. -L.; Wicke, S. E.; Bacsa, J.; Dunbar, K. R.; Turro, C. *Inorg. Chem.* **2004**, *43*, 8510−8519.

(13) Sigman, D. S.; Graham, D. R.; Aurora, V. D.; Stern, A. M. *J. Biol. Chem.* **1979**, *254*, 12269−12272.

(14) Spassky, A.; Sigman, D. S. *Biochemistry* **1985**, *24*, 8050−8056.

(15) Sigman, D. S.; Mazumder, A.; Perrin, D. M. *Chem. Rev.* **1993**, *93*, 2295−2316.

(16) Hudson, B. P.; Barton, J. K. *J. Am. Chem. Soc.* **1998**, *120*, 6877−6888.

(17) Maheswari, P. U; Roy, S.; Dulk. H. D.; Barends, S.; Wezel, G. V.; Kozlevcar, B.; Gamez, P.; Reedijk, J. *J. Am. Chem. Soc.* **2006**, *128*, 710−711.

(18) Chikira, M.; Tomizava, Y.; Fukita, D.; Sugizaki, T.; Sugawara, N.; Yamazaki, T. Sasano, A.; Shindo, S.; Palaniandavar, M.; Anthroline, W. E. *J. Inorg. Biochem.* **2002**, *89*, 163−173.

(19) (a) Barceló-Oliver, M.; García-Raso, Á.; Terrón, Á.; Molins, E.; Prieto, M. J.; Moreno, V.; Martínez, J.; Lladó, V.; López, I.; Gutiérrez, A.; Escribá, P. V. *J. Inorg. Biochem.* **2007**, *101*, 649−659. (b) García-Raso, Á.; Fiol, J. J.; Adrover, B.; Moreno, V.; Mata, I.; Espinso, E.; Molins, E. *J. Inorg. Biochem.* **2003**, *95*, 77−86. (c) Selvakumar, B.; Rajendiran, V.; Maheswari, P. U.; Evans, H. S.; Palaniandavar, M. *J. Inorg. Biochem.* **2006**, *100*, 316−330. (d) Reddy, P. A. N.; Nethaji, M.; Chakravarty, A. R. *Eur. J. Inorg. Chem.* **2004**, 1440−1446.

(20) Ranford, J. D.; Sadler, P. J; Tocher, D. A. *Dalton Trans.* **1993**, 3393−3399.

(21) Zhang, S.; Zhu, Y.; Tu, C.; Wei, H.; Yang, Z.; Lin, L.; Ding, J.; Zhang, J.; Guo, Z. *J. Inorg. Biochem.* **2004**, *98*, 2099−2106.

(22) (a) Sielecki, T. M.; Boylan, J. F.; Benfield, P. A.; Trainor, G. L. *J. Med. Chem.* **1999**, *43*, 1−18. (b) Zang, Z.; Jin, L.; Qian, X.; Wei, M.; Wang, Y.; Wang, J.; Yang, Y.; Xu, Q.; Xu, Y.; Liu, F. *ChemBioChem* **2007**, *8*, 113−121.

(23) Siu, P. K. -M.; Ma, D. -L.; Che, C. M. *Chem. Commun.* **2005**, 1025−1027.

(24) (a) Mahadevan, S.; Palaniandavar, M. *Inorg. Chem.* **1998**, *37*, 693−700. (b) Raja, A.; Rajendiran, V.; Maheswari, P. U.; Balamurugan, R.; Kilner, C. A.; Halcrow, M. A.; Palaniandavar, M. *J. Inorg. Biochem.* **2005**, *99*, 1717−1732.

Scheme 1.

Scheme 1. Possible Coordination Geometries of Simple and Mixed-Ligand Copper(II) Complexes of H(tdp) and Structures of Diimine (N–N) Coligands
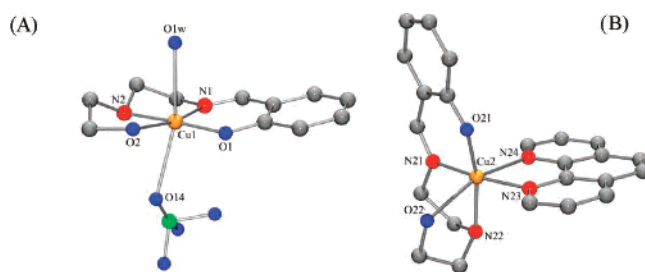

Figure 1. Ball-and-stick representation of the crystal structure of [Cu-(tdp)(ClO$_4$)]·0.5H$_2$O (**1**) (A) and [Cu(tdp)(phen)](ClO$_4$)·CH$_3$OH (**3**) (B); atoms are shown as spheres of arbitrary diameter. Hydrogen atoms are omitted for clarity.

those in tmp, would provide a hydrophobic recognition element.[19c] The effect of variation of the nature of coligand, the number and size of aromatic rings, and hydrophobicity on DNA and protein binding and DNA cleavage by the complexes has been investigated, and attempts have been made to understand the chemical principles underlying site-specific DNA and protein recognition and then see whether they can be used as promising drugs for cancer. Further, because cervical cancer is the second most prevalent cancer in women worldwide, 500 000 new cases are diagnosed every year,[25a] and the current drug cisplatin is limited by its side-effects and cellular resistance,[25b] we prefer to screen the cytotoxicity of the complexes with human epidermoid cervical carcinoma cell line (ME180). The dpq complex binds to CT DNA more strongly than other complexes and causes significant cleavage of supercoiled pBR322 DNA in the absence of an added reductant. Also, the tmp complex exhibits cytotoxicity higher than the other diimine complexes and more interestingly, it is more potent than the currently used drugs cisplatin and mitomycin C against cervical cancer cell line. Further, it mediates the arrest of S and G$_2$/M phases in the cell cycle progression at 24 h harvesting time, which progress into apoptosis.

Results and Discussion

Synthesis and Structures of Complexes. The complex [Cu(tdp)(ClO$_4$)]·0.5H$_2$O (**1**), where H(tdp) is the tetradentate ligand 2-[(2-(2-hydroxyethylamino)ethylimino)methyl]phenol, and the mixed ligand complexes [Cu(tdp)(diimine)]ClO$_4$, where diimine = 2,2′-bipyridine (bpy) (**2**), 1,10-phenanthroline (phen) (**3**), 3,4,7,8-tetramethyl-1,10-phenanthroline (3,4,7,8-tmp) (**4**), and dipyrido-[3,2-*d*:2′,3′-*f*]-quinoxaline (dpq) (**5**), have been isolated from methanloic solutions containing hexahydrated copper(II) perchlorate as the starting material (Scheme 1). All the complexes were obtained in good yields and characterized by using elemental analysis, UV–Vis, and EPR spectral techniques. The formulation of the complexes is confirmed by determination of the X-ray crystal structures of **1** and **3**. While all the complexes are soluble in 10% DMF/5 mM Tris-HCl/50 mM NaCl buffer at pH 7.1, **1**–**3** are soluble in water.

Description of Structures of [Cu(tdp)(ClO$_4$)]·0.5H$_2$O- (1) and [Cu(tdp)(phen)](ClO$_4$)·CH$_3$OH (3). The ORTEP representation of the structures of **1** and **3** including the atom-numbering scheme are shown in Figure 1A and B, respec-

tively, and the selected bond lengths and bond angles are listed in Tables S1 and S2, respectively. The asymmetric unit cell of **1** consists of two crystallographically independent complex molecules A and B with two different coordination geometries.[26] In the molecule A, Cu(II) is located at the center of a distorted octahedral coordination environment, and the phenolate (O1) and ethanolic (O2) oxygen atoms and the secondary amine (N2) and imine (N1) nitrogen atoms of the phenolate ligand occupy the corners of the basal plane. A water molecule (O1W) and a perchlorate oxygen atom (O14) occupy the axial positions at distances longer than the equatorial ones, which is a consequence of the tetragonal distortion caused by Jahn–Teller effect (one electron in d$_{x^2-y^2}$ orbital). Further, the axial Cu–O1W bond (2.539 Å) is slightly shorter than the axial Cu–O14 bond (2.550 Å). The Cu–N$_{amine}$ bond (1.985 Å) is longer than the Cu–N$_{imine}$ bond (1.939 Å), which is expected for the sp^3 and sp^2 hybridizations of the amine and imine nitrogen atoms, respectively. The value of the structural index,[27] τ, of 0.13 [$\tau = (\beta - \alpha)/60$, where α = O3–Cu2–N22 = 174.2° and β = N21–Cu2–O4 = 166.4°; for perfect square pyramidal and trigonal bipyramidal geometries the τ values are zero and unity, respectively] for the molecule B reveals that it possesses, in contrast to A, a square-pyramidal coordination geometry with Cu(II) coordinated to the phenolate (O3) and ethanolic (O4) oxygen atoms, and the secondary amine (N21) and imine (N22) nitrogen atoms of the phenolate ligand occupy the corners of the basal plane. A perchlorate oxygen atom (O21) occupies the axial position at a distance longer than the equatorial ones, as in molecule A.

The asymmetric unit cell of complex **3** consists of two crystallographically independent molecules of the same complex. The corners of CuN$_3$O basal plane of the octahedral coordination sphere of **3** is occupied by the phenolate oxygen (O21), the imine (N21) and amine (N22) nitrogens of the Schiff base ligand H(tdp), and one of the nitrogen atoms (N23) of phen. The axial positions are occupied by the ethanolic oxygen atom (O22) of the ligand at a distance (Cu–O22 = 2.5120 Å) longer than that for the equatorial oxygen

(25) (a) Parker, S. H.; Tong, T.; Bolden, S.; Winko, P. A. *Cancer J. Clin.* **1996**, *46*, 5–27. (b) Gately, D. P.; Howell S. B. *Br. J. Cancer* **1993**, *67*, 1171–1174.

(26) Sanni, S. B.; Behm, H. J.; Beurskens, P. T.; Van Albada, G. A.; Reedijk J.; Lenstra, A. T. H.; Addison, A. W.; Palaniandavar, M. *Dalton Trans.* **1988**, 1429–1435.

(27) Addison, A. W.; Rao, T. N.; Reedijk, J.; van Rijn, J.; Veschoor, G. C.; *J. Chem. Soc., Dalton Trans.* **1984**, 1349–1356.

atom (Cu−O21 = 1.9402 Å) and the second nitrogen atom (N24) of phen at a distance (Cu−N24 = 2.348 Å) longer than that for the equatorial one (Cu−N23 = 2.018 Å), which is a consequence of the tetragonal distortion caused by Jahn−Teller effect (one electron in $d_{x^2-y^2}$ orbital). The Cu−N$_{amine}$ bond (Cu−N22 = 2.057 Å) is longer than the Cu−N$_{imine}$ bonds (Cu−N21 = 1.953 Å, Cu−N23 = 2.018 Å), as in complex **1** (cf. above) (Table S2). The geometries around copper(II) in both **1** and **3** are best described as distorted octahedral as revealed by the values of the bond angles (**1** N1−Cu−O2 = 167.54°, N2−Cu−O1 = 177.17°, O1−Cu1−O2 = 95.30°; **3** N21−Cu−N23 = 171.37°, O21−Cu−N22 = 165.76°, O21−Cu−N24 = 106.61°), which deviate from those (90 and 180°) expected for an ideal octahedral geometry. Interestingly, the incorporation of the strong chelating phen ligand in the coordination sphere of **1** displaces the equatorially coordinated ethanolic oxygen of H(tdp) to default[28a] to the more weakly bound axial position in **3**.

Solution Structures. In 10% DMF/5 mM Tris-HCl/50 mM NaCl buffer at pH 7.1 solutions, the complexes **1**−**4** exhibit only one broad band in the visible region (620−650 nm) with very low absorptivities (Table S3), revealing a slightly distorted square-based Cu(II) coordination geometry, which is consistent with the X-ray crystal structures of **1** and **3** and the EPR spectral data of the complexes (see below). Complex **5** exhibits only one broad band around 630 nm in DMF solution. The observation of the PhO$^-$ → Cu-(II) LMCT transition[28b] as an intense band in the range of 325−353 nm (ϵ_{max} = 3255−8955 M^{-1} cm^{-1}) for all the complexes reveals the involvement of phenolate oxygen atom in coordination in solution. The frozen solution EPR spectra of the complexes are axial with $g_\parallel > g_\perp > 2.0$ and G^{29a} = $[(g_\parallel - 2)/(g_\perp - 2)]$ = 3.6−4.2, confirming that the square-based geometries of the complexes, as observed in the X-ray crystal structures of **1** and **3,** are retained in solution. A square-based CuN$_4$ chromophore is expected to show a $g_\parallel$ value of around 2.200 and an $A_\parallel$ value of 180−200 × 10^{-4} cm^{-1}, and the replacement of a nitrogen atom in this chromophore by an oxygen atom is expected to increase the $g_\parallel$ value and decrease the $A_\parallel$ value. On the other hand, distortion from square planar coordination geometry would increase the $g_\parallel$ value and decrease the $A_\parallel$ value. The observed $g_\parallel$ (2.215−2.235) and $A_\parallel$ (186−197 × 10^{-4} cm^{-1}) values are consistent with the presence of a square-based CuN$_2$O$_2$ chromophore with no significant distortion from planarity[29b] ($g_\parallel/A_\parallel$ = 114−120 cm) as in the X-ray crystal structures of **1** and **3**.

DNA Binding Studies. Absorption Spectral Studies. Changes in the $\pi \rightarrow \pi^*$ transition of **1**−**5** in 10% DMF/5 mM Tris-HCl/50 mM NaCl buffer at pH 7.1 were determined as a function of added DNA concentration, and the typical

(A)

(B)

[DNA], M
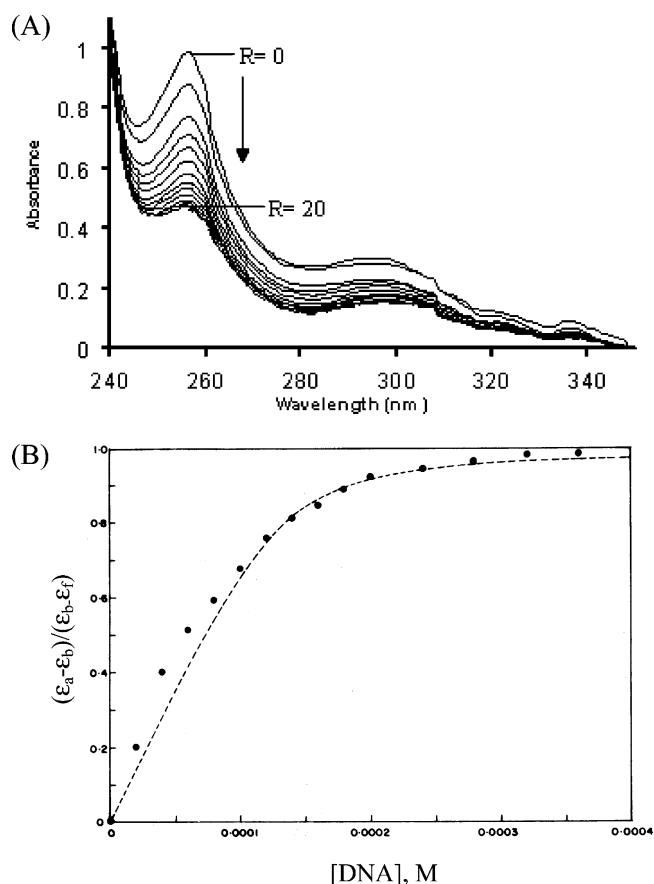
Figure 2. (A) Absorption spectra of [Cu(tdp)(dpq)](ClO$_4$) (2 × 10^{-5} M) in 10% DMF/5 mM Tris-HCl/50 mM NaCl buffer at pH 7.1 (R = [DNA]/ [complex] = 0) and presence (R = 1−20) of increasing amounts of DNA. (B) Plot of ($\epsilon_a - \epsilon_b$)/($\epsilon_b - \epsilon_f$) vs [DNA] for [Cu(tdp)(dpq)](ClO$_4$). The best fit line, superimposed on the data, according to eqs 1a and 1b yields K_b = 9.0 × 10^5 M^{-1} and s = 3.3.

titration curve for **5** is shown in Figure 2. A decrease in molar absorptivity (hypochromism, 27−54%, Table 1) for all the complexes with significant red-shifts for **1** (11 nm) and **2** (6 nm) are observed. These spectral changes are typical of a complex bound to DNA through intercalation involving partial insertion of the aromatic chromophore of the diimine ligands in between the base pairs of DNA.[30−32] The values of intrinsic binding constants K_b (Table 1) determined from these changes follow the order **5** > **4** > **3** > **2**, which is in conformity with the observed trend in hypochromism. The K_b value of the dpq complex **5** is the highest, which is expected because the extended aromatic ring of dpq inserted into the base stacks of DNA more deeply than the phen ring of **3**.[33] Further, the incorporation of methyl groups at the 3,4,7,8-positions on the phen ring would be expected to hinder the partial intercalation of the phen ring leading to a lower DNA binding affinity for **4**. However, a higher K_b value is obtained suggesting a strong hydrophobic interaction between the methyl groups of tmp ligand in **4** and the

(28) (a) Palaniandavar, M.; Pandiyan, T.; Lakshminarayanan, M.; Manohar, H. *Dalton Trans.* **1995**, 455−461. (b) Vaidyanathan, M.; Viswanathan, R.; Palaniandavar, M.; Balasubramanian, T.; Prabhaharan, P.; Muthiah, P. T. *Inorg. Chem.* **1998**, *37*, 6418−6427.

(29) (a) Hathaway, B. J.; Billing, D. E. *Coord. Chem. Rev.* **1970**, *5*, 143−207. (b) Sakaguchi, U.; Addison, A. W. *J. Chem. Soc., Dalton Trans.* **1979**, 600−608.

(30) Tysoe, S. A.; Morgan, R. J.; Baker, A. D.; Strekas, T. C. *J. Phys. Chem.* **1993**, *97*, 1707−1717.

(31) Kelly, J. M.; Tossi, A. B.; McConnell, D. J.; Strekas, T. C. *Nucleic Acids Res.* **1985**, *13*, 6017−6034.

(32) Haworth, I. S.; Elcock, A. H.; Freemann, J.; Rodger, A.; Richards, W. G. *J. Biomol. Struct. Dyn.* **1991**, *9*, 23−43.

(33) Hiort, C.; Lincoln, P.; Norden, B. *J. Am. Chem. Soc.* **1993**, *115*, 3448−3454.

Table 1. Absorption Spectral Properties of Cu(II) Complexes Bound[a] to CT DNA

complex		$\lambda_{\text{max (nm)}}$	R	change in abs	$\Delta\epsilon$ (%)	red shift (nm)	$K_b \times 10^5$ (M^{-1})	s^b
				ligand-based				
[Cu(tdp)]$^+$	1	264	20	hypo- and hyperchromism	53	11	c	
[Cu(tdp)(bpy)]$^+$	2	269	20	hypochromism	33	6	0.071 ± 0.005	0.5
[Cu(tdp)(phen)]$^+$	3	276	20	hypochromism	27	1	0.90 ± 0.03	1.6
[Cu(tdp)(tmp)]$^+$	4	269	20	hypochromism	49	1	7.0 ± 0.2	2.1
[Cu(tdp)(dpq)]$^+$	5	256	20	hypochromism	54	1	9.0 ± 0.1	3.3

[a] Measurements were made at $R = 20$, where $R = $ [DNA]/[Cu complex]; concentration of copper(II) complex = 4×10^{-5} M (**1** and **2**) and 2×10^{-5} M (**3**, **4** and **5**). [b] Binding site size in base pairs. [c] Binding constant was not calculated because spectral changes are not uniform.

hydrophobic interior accessible in DNA.[34] The Schiff base ligand would encourage intercalation of dpq in the minor groove (cf. below) by engaging in hydrogen-bonding interactions between coordinated −NH− and −OH with the functional groups positioned on the edge of DNA bases.[34−36]

Ethidium Bromide Displacement Assay. Upon addition of complexes **1**−**5** to DNA ($R = $ [DNA]/[complex] = 1) pretreated with ethidium bromide ([DNA]/[EthBr]) = 1), the emission intensity of DNA-bound EthBr decreases (Figure S1). From the plot of these intensities against complex concentration, the values of apparent DNA binding constant (K_{app}) were calculated[37] using the equation

$$K_{\text{EthBr}}[\text{EthBr}] = K_{\text{app}}[\text{complex}]$$

where K_{EthBr} is 1.0×10^7 M^{-1}, the concentration of EthBr is 12.5 μM, and the concentration of the complex is that used to obtain a 50% reduction of fluorescence intensity of EthBr. The DNA binding abilities of the complexes follow the order **5** ($K_{\text{app}} = 25.0 \times 10^5$ M^{-1}) > **4** (12.5×10^5 M^{-1}) > **3** (10.0×10^5 M^{-1}) > **2** (7.8×10^5 M^{-1}) > **1** (4.6×10^5 M^{-1}), which is consistent with the results from absorption spectral studies (cf above). Both the electron transfer from excited EthBr to copper(II) and the displacement of EthBr would account for the highest K_{app} value of the dpq complex **5** with the highest Cu(II)/Cu(I) redox potential (cf. below) and DNA binding affinity (cf. above). Similarly, phen complex **3** with $E_{1/2}$ values higher than the tmp complex **4** would be expected to show a K_{app} value higher than that of **4**. But the observation of a higher K_{app} value for the latter indicates the predominant hydrophobic interaction of **4** with DNA.

Circular Dichroism Spectral Study. The observed CD spectrum of calf thymus DNA (Figure 3) consists of a positive band at 275 nm (UV, λ_{max} = 258 nm) caused by base stacking and a negative band at 245 nm caused by helicity, which are characteristic of DNA in right-handed B form.[38] When the DNA was incubated with **1**−**5** at a 1/R value of 1 ($R = $ [Cu complex]/[DNA]), changes in both the positive and negative signals of DNA were observed, but for **3**−**5** only. The phen (**3**) and dpq (**5**) complexes show changes in both the positive and negative bands (Table S4,
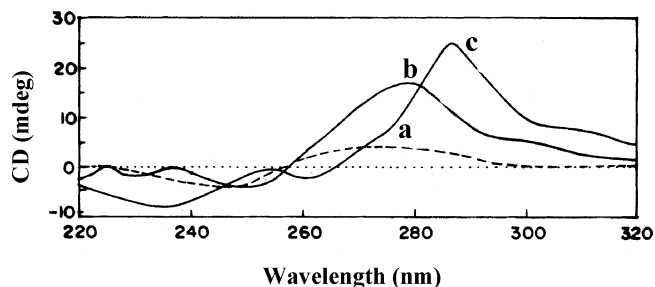
Figure 3. Circular dichroism spectra of CT DNA in 10% CH$_3$CN/5 mM Tris-HCl/50 mM NaCl buffer at pH 7.1 and 25 °C the absence (a) and presence (b) of [Cu(tdp)(phen)](ClO$_4$) and [Cu(tdp)(tmp)](ClO$_4$) (c) at 1/R value of 1.

Figure 3), which are characteristic of partial intercalative interaction of the heterocyclic rings of the complexes. Interestingly, high-intensity bands for **3**−**5** resulting from induced CD (ICD) on the broad positive band at 279, 287, and 262 nm, respectively, which correspond to positions of their UV absorption bands, are observed. The higher red-shift (15 nm) with a large decrease in intensity of the DNA helicity band and that (∼14 nm) with increase in intensity in the positive band of **4** (Figure 3) are consistent with a B to A conformational change of DNA on binding of the complex with the methyl groups on tmp coligand effectively placed in DNA grooves. Similar observations made for [Cu-(imda)(5,6-dmp)] (imda = iminodiacetate, 5,6-dmp = 5,6-dimethyl-1,10-phenanthroline),[19c] [Co(bpy)$_2$(imp)]$^{3+}$, and [Ru(NH$_3$)$_4$(imp)]$^{2+}$ (imp = imidazo[4,5-f]-1,10-phenanthroline) bound to CT DNA have been ascribed to the B to A conformational change.[39a,b] When **3** and **4** interact with poly-(GC)$_{12}$, poly(AT)$_{12}$, and d(CGCGATCGCG)$_2$ (1/R = 4) changes in CD spectra similar to those observed for CT DNA are observed. Also, a blue shift (7 nm) for the helicity band and a red-shift (7 nm) for the positive band were observed for **4** bound to poly(AT)$_{12}$ revealing that the complex with bulky tmp ligand binds selectively with the polynucleotide, which contains more spacious major grooves (Table S5, Figure S2).[39c]

Viscometry Studies. The values of relative specific viscosity (η/η_0)$^{1/3}$, where η and η_0 are the specific viscosities of DNA in the presence and absence of the complexes, were determined and plotted against values of 1/R ($R = $ [NP]/[Cu complex], Figure S3). A small to large increase in

(34) Chan, H. L.; Liu, H. Q.; Tzeng, B. C.; You, Y. S.; Peng, S. M.; Yang, M.; Che, C. M. *Inorg. Chem.* **2002**, *41*, 3161−3171.
(35) Boom, V.; Rich, A. *Biochemistry* **1985**, *24*, 237−240.
(36) Maheswari, P. U.; Palaniandavar, M. *J. Inorg. Biochem.* **2004**, *98*, 219−230.
(37) Lee, M.; Rhodes, A. L.; Wyatt, M. D.; Forrow S.; Hartley, J. A. *Biochemistry* **1993**, *32*, 4237−4245.
(38) Collins, J. G.; Shields, T. P.; Barton, J. K. *J. Am. Chem. Soc.* **1994**, *116*, 9840−9846.
(39) (a) Tamil Selvi, P.; Murali, M.; Palaniandavar, M.; Kockerling, M.; Henkel, G. *Inorg. Chim. Acta* **2002**, *340*, 139−146. (b) Maheswari, P. U.; Palaniandavar, M. *Inorg. Chim. Acta* **2004**, *357*, 901−912. (c) Maheswari, P. U.; Rajendiran, V.; Parthasarathi, R.; Subramanian, V.; Palaniandavar, M. *J. Inorg. Biochem.* **2006**, *100*, 3−17.

(A)

(B)
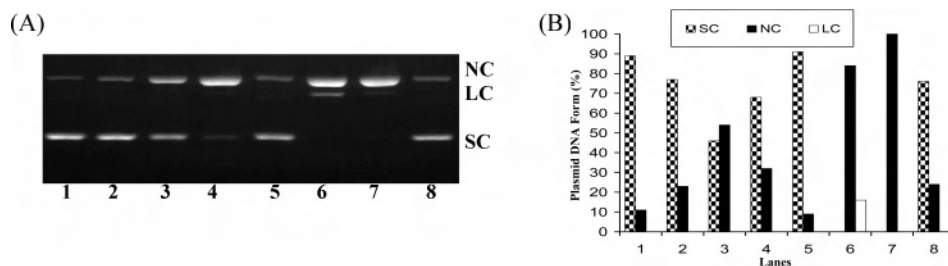
Figure 4. (A) Gel electrophoresis diagram showing the hydrolytic cleavage of supercoiled pBR322 DNA (40 μM in base pair) by complexes **1**−**5** (120 μM) in 10% DMF/5 mM Tris-HCl/50 mM NaCl buffer at pH 7.1 and 37 °C with an incubation time of 4 h: lane 1, DNA; lane 2, DNA + **1**; lane 3, DNA + **2**; lane 4, DNA + **3**; lane 5, DNA + **4**; lane 6, DNA + **5**; lane 7, DNA + [Cu(dpq)$_2$(H$_2$O)]$^{2+}$; lane 8, DNA + Cu(ClO$_4$)$_2$·6H$_2$O. Forms SC, NC, and LC are supercoiled, nicked circular, and linear circular DNA, respectively. (B) Relative amounts of the different DNA forms in presence of **1**−**5**.

viscosity of DNA is observed for almost all the complexes, and the ability of the complexes to increase the viscosity of DNA follows the order **5** > **4** ≈ **3** > **2** ≈ **1**. The increase in viscosity of DNA by **5** is the highest among all the complexes but lower than that for the potential intercalator, namely, ethidium bromide,[40] suggesting insertion of planar dpq ring into the base pairs of DNA as discussed above. It is obvious that the strong hydrophobic interaction of the coordinated tmp coligand with the interior of the DNA grooves is also effective in increasing the length of DNA biopolymer. The viscosity enhancement for the phen complex **3**, which is higher than the bpy complex **2**, is traced to the presence of the central planar aromatic ring in the former. Thus, all these observations suggest that it is the central aromatic rings of dpq and phen, which are involved in partial intercalative mode of DNA binding.

Electrochemical Studies. The Cu(II)/Cu(I) redox potentials of complexes **1**−**5** (Table S6) display significant variations depending upon the π-delocalized diimines: **5** > **3** > **4** ≈ **2** ≈ **1**; obviously, the π-delocalization of electron density from copper into the extended planar ring of dpq destabilizes Cu(II) oxidation state. When the interaction of the complexes with DNA was studied using differential pulse voltammetry, all the complexes, except **2**, display a decrease in cathodic peak current in the presence of excess of DNA (R = 3). The interesting increase in peak current for **2** suggests the involvement of catalytic reactions. Also, the shifts in $E_{1/2}$ to negative values for **1**, **3**, and **5** suggest that Cu(II) rather than Cu(I) form of the complexes bind to DNA more strongly. On the other hand, the positive shifts for **2** and **4** suggest that Cu(I) form of the complexes display binding affinities higher than those of the Cu(II) form.

DNA Cleavage Studies. DNA Cleavage without Added Reductant. To assess the DNA cleavage ability of the complexes supercoiled (SC) pBR322 DNA (40 μM in base pairs) was incubated with varying concentrations of **1**−**5** in 10% DMF/5 mM Tris-HCl/50 mM NaCl buffer at pH 7.1 (Figure 4A and B) for 4 h without addition of a reductant. Upon gel electrophoresis of the reaction mixture, a concentration-dependent DNA cleavage was observed. At 0.12 mM concentration, **2**, **3**, and **5** cause DNA cleavage, while **1**, **4**, and Cu(ClO$_4$)$_2$·6H$_2$O do not. Complex **5** has a higher

percentage of DNA cleavage with 84% nicked circular (NC, Form II) and 16% linear circular (LC, Form III), whereas **2** and **3** produce 54 and 91% of NC, respectively, but no LC. At a higher concentration of 0.25 mM, **5** produces complete cleavage of SC to NC (100%), with no LC (Figure S4A, Table S7), whereas **2** and **3** yield 63 and 60% of NC but not LC form. respectively. At a still higher complex concentration (1.0 mM), **3**, **4**, and **5** cause complete cleavage into both NC and LC forms, while **1** and **2** produce 66 and 68% NC, respectively, and 23% LC (Figure S4B, Table S7). All three forms are visible on the gel, indicating that **1** and **2** are involved in double-strand DNA cleavage to generate the LC form before converting all of the SC form to NC DNA through single-strand breaking.[41] This is interesting because **1** and **4** fail to cleave DNA at lower concentrations. To evaluate the role of the primary ligand, the cleavage abilities of [Cu(tdp)(diimine)]$^+$ at the 0.12 mM concentration have been compared with those of the corresponding bis-diimine complexes. The complex [Cu(dpq)$_2$(H$_2$O)](ClO$_4$)$_2$ has been already reported[42] to hydrolytically cleave DNA under conditions identical to the present one to yield 100% NC but not LC form. This is in contrast to **5**, which cleaves DNA to give both NC and LC forms. Also, the complexes **2** and **3** produce a DNA cleavage with an efficiency higher than that of their corresponding bis-complexes ([Cu(bpy)$_2$(H$_2$O)]-(ClO$_4$)$_2$, 31% NC; [Cu(phen)$_2$(H$_2$O)](ClO$_4$)$_2$, 68% NC) under the present conditions (Figure S5). At 0.12 mM concentration, **1** causes no significant DNA cleavage; however, incorporation of diimines as coligands in **1** modifies the structural, spectral, and electrochemical properties of the ternary complexes [Cu(tdp)(diimine)]$^+$ (see above) and hence tunes their DNA binding affinity and cleavage ability to different extents depending upon the coligand. Thus complex **5** with the coligand dpq as a recognition element (partial intercalation) exhibits the strongest DNA-binding affinity and cleaves DNA effectively. Similar enhanced cleavage activity of copper(II) complexes showing stronger DNA-binding affinity resulting from a partially intercalating dpq ligand

(40) Gabbay, E. J.; Scofield, R. E.; Baxter, C. S. *J. Am. Chem. Soc.* **1973**, *95*, 7850−7857.

(41) Melvin, M. S.; Tomlinson, T.; Saluta, G. R.; Kucera, K. L.; Lindquist, L.; Manderville, R. A. *J. Am. Chem. Soc.* **2000**, *122*, 6333−6334.

(42) (a) Dhar, S.; Reddy, P. A. N.; Chakravarty, A. R. *Dalton Trans.* **2004**, 697−698.
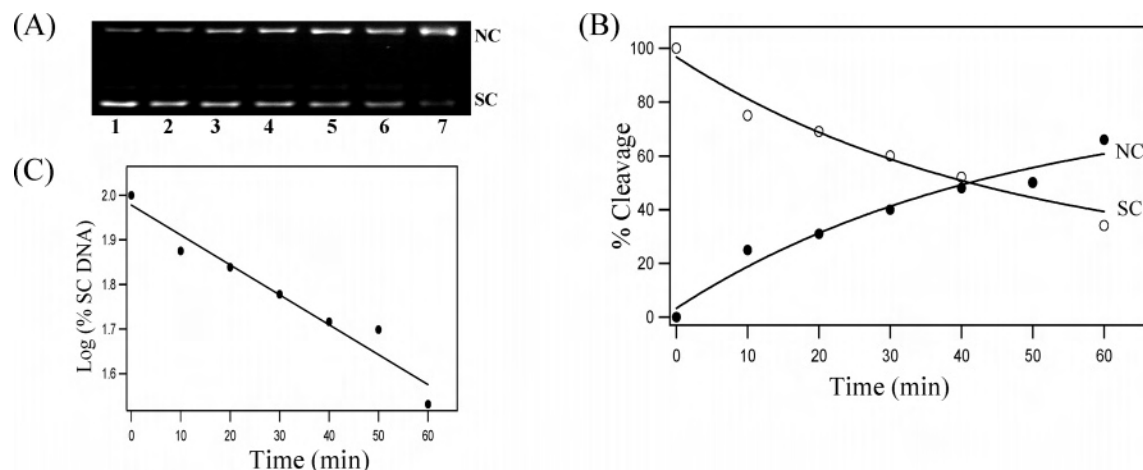
Figure 5. (A) Time course of supercoiled pBR322 DNA (40 μM in base pair) cleavage by complex 5 (50 μM) in a 10% DMF/5 mM Tris-HCl/50 mM NaCl buffer at pH 7.1 and 37 °C with incubation times of 0, 10, 20, 30, 40, 50, and 60 min for lanes 2−7. (B) Hydrolytic cleavage of supercoiled pBR322 DNA showing the decrease in form I (SC DNA) and the formation of form II (NC DNA) with incubation time using 50 μM concentration of **5**. (C) the plot shows log(% SC DNA) vs time for complex **5** (50 μM) for an incubation period of 0−60 min.

has been observed previously.[43] On the other hand, complex **4** with the coligand tmp as a recognition element (groove binding) displays a stronger DNA binding than its phen analogue and a lower DNA cleavage ability, possibly, because it causes a conformational change on DNA. The effect of concentration of complexes on DNA cleavage rate was studied typically for complex **5** (which shows the highest cleavage activity) using a constant concentration of SC pBR322 DNA (40 μM, in base pair) under "pseudo-Michaelis−Menten" kinetic conditions with an incubation period of 60 min (Figure S6). The rates of cleavage were calculated, and the kinetic parameters were derived from a plot of k_{obs} versus concentration of complex. The value of K_{cat}, which is the maximum rate of cleavage observed upon varying catalyst concentration, is 5.47 ± 0.10 h^{-1} under the present experimental conditions, and the corresponding value of K_M is 32.6 μM. Thus the cleavage rate enhancement is 1.5×10^8 in comparison with the uncatalyzed rate of cleavage of ds-DNA (3.6×10^{-8} h^{-1}).[44] This rate enhancement is significantly higher than those reported for transition metal-based synthetic hydrolases.[44] However, the observed value of the specificity constant ($K_{cat}/K_M = 1.68 \times 10^5$ h^{-1} M^{-1}) is lower than that (4.8×10^5 h^{-1} M^{-1}) for Cu^{2+}-neamine.[44] Further, the DNA cleavage has also been followed under "true Michaelis−Menten" kinetic conditions using a constant catalyst concentration (50 μM) and various substrate concentrations (20−160 μM in base pair) with an incubation period of 60 min. Interestingly, the k_{obs} values obtained sharply increase and then decrease with increase in DNA concentration, which does not correspond to true Michaelis−Menton saturation behavior. Although no perfect saturation behavior is exhibited, the maximum k_{obs} value (3.7 h^{-1}), obtained from the plot, is taken as V_{max} (Figure S7), and the value of K_{cat} (0.074 h^{-1}) obtained under the present conditions (20 μM DNA concentration) corresponds to a 2.1 ×

10^6-fold rate enhancement over uncatalyzed DNA hydrolysis. This is remarkable because no mononuclear copper complex has been found, thus far, to exhibit such a behavior. It appears that a larger number of binding sites are available at higher DNA concentrations, and the complex molecules irreversibly bind to DNA with no free complex being available to get self-activated. The kinetics of DNA cleavage catalyzed by **5** has been also studied. The extent of cleavage is found to vary exponentially with incubation time, and the cleavage follows pseudo-first-order kinetics. The kinetic plots show that both the formation of the NC form and the degradation of SC DNA versus time follow pseudo-first-order kinetics and fit well into a single-exponential curve, at 0.05 (Figure 5) and 1.0 mM (Figure S8) complex concentrations. The plot of log(% SC DNA) with time gives a linear fit at a 0.05 mM concentration of complex. It is remarkable that at 1.0 mM concentration, the cleavage is completed within 30 s.

For the complexes **3** and **5**, which show efficient DNA cleavage, mechanistic studies were performed. The cleavage reactions were carried out in the absence of a reductant by addition of a variety of radical scavengers like DMSO (hydroxyl radical), NaN$_3$ (singlet oxygen), and superoxide dismutase (super oxide) (Figure S9A). Because the reaction was not inhibited, the possibility of free radicals being involved as the active species in the cleavage is excluded. When the cleavage reaction was performed with the addition of catalase enzyme, no inhibition of cleavage is observed (Figure S9A), ruling out the participation of H$_2$O$_2$ in the cleavage. Also, under an argon atmosphere, both the complexes **3** and **5** exhibit DNA cleavage efficiencies slightly higher than those in air (Figure S9A), revealing the non-involvement of molecular oxygen in the cleavage. All these observations support the hydrolytic DNA cleavage mechanism. To collect further evidence for the hydrolytic cleavage mechanism additional cleavage experiments were conducted using a T4 ligase enzymatic assay. The ligation experiment involves incubation of complex **3** with pBR322 plasmid DNA for 4 h and then aliquoting the cleaved fragments into two eppendorfs. One of the aliquots was subjected to ligation

(43) (a) Thomas, A. M.; Nethaji, M.; Mahadevan, S.; Chakravarty, A. R. *J. Inorg. Biochem.* **2003**, *94*, 171−178. (b) Santra, B. K.; Reddy, P. A. N.; Neelakanta, G.; Mahadevan, S.; Nethaji, M.; Chakravarty, A. R. *J. Inorg. Biochem.* **2002**, *89*, 191−196.

using T4 DNA ligase at 16 °C for 24 h. When the linearized plasmid Lambda/Hind III and pUC18/Sau 3A I-pUC18/Taq I digest was used as a positive control, it was found to be religated. In contrast, the copper-mediated cleavage products were not religated (Figure S9B). It appears that the hydrolytic cleavage products do not possess strictly matched ends suitable for religation.[45] The addition of an excess of sodium chloride (250 mM) inhibits, but only slightly, the cleavage by **3** and **5** (Figure S10), clearly indicating that partial intercalation of coordinated phen and dpq in the minor groove plays an important role in the intimate DNA binding of the complexes. It is likely[46] that the hydrolytic DNA cleavage by **1**−**5** occurs by the nucleophilic attack of copper-bound ligand ethanolato oxygen site on DNA phosphate bonds. However, in the present study, no evidence for the involvement of any diffusible radical could be observed. The DNA cleavage observed under argon and in the presence of catalase rules out the need for dioxygen and H_2O_2, respectively. The effective partial intercalation of the dpq co-ligand of **5** would enable the copper(II)-bound ethanolato oxygen group to be brought closer to the deoxyl ribose rings, which is supported, possibly, by the hydrogen-bonding interaction of the −NH− and hydrophobic interaction of the alkyl chains of tdp ligand.

DNA Cleavage with Added Reductant. To ascertain whether any adventitious reducing agents present in the reaction mixture could account for the increased DNA degradation by **1**−**5** (Figure S11A, Table S8) cleavage reactions were performed in the presence of O_2 by deliberate addition of the reducing agent ascorbic acid to the reaction mixture containing supercoiled pBR322 DNA in a medium of 10% DMF/5 mM Tris-HCl/50 mM NaCl buffer at pH 7.1. In the control experiment using ascorbic acid in the absence of a complex, no cleavage of DNA was observed. Interestingly, the dpq (**5**) and phen (**3**) complexes convert the SC form to NC and LC forms without any evidence for a direct double-strand DNA cleavage (Figure S12), while **1**, **2**, and **4** convert the SC form only to the NC form. The intense nuclease activity of **5** is apparently caused by enhanced stabilization of the Cu(I) (cf. above) species formed upon its reduction by ascorbic acid. The DNA cleavage efficiency of **5** is also higher than that already reported[43b] for the corresponding bis-complex [Cu(dpq)$_2$(H$_2$O)](ClO$_4$)$_2$. This is the result of tuning of the Cu(II)/Cu(I) redox potential of **5** to a less-positive value by incorporation of a coordinated phenolate ligand to confer efficient DNA cleavage activity. When a hydroxyl radical scavenger like DMSO was added to the reaction mixture, the cleavage reactions were inhibited for all the ternary complexes (Figure S11B), revealing that a freely diffusible hydroxyl radical is the reactive oxygen species (ROS) directly responsible for initiation of the cleavage reaction. Again, the cleavage activity of the complexes was inhibited in the presence of a minor groove

binder like distamycin suggesting that **1**−**5** bind to DNA in the minor groove (Figure S13).

Photoinduced DNA Cleavage. The DNA cleavage activities of **1**−**5** at a 25 μM concentration were studied using SC pBR322 DNA (40 μM in base pair) in 10% DMF/5 mM Tris-HCl/50 mM NaCl buffer at pH 7.1 and upon irradiation with UV light of 365 nm (Figure S14A, Table S9). Of all the complexes, only **5** displays cleavage of SC DNA to 89% NC form and 3% LC form. Interestingly, **5** involves double-strand DNA cleavage to generate the LC form, before converting all of SC form to NC DNA through single-strand breaks.[41] On the other hand, the corresponding bis-complex [Cu(dpq)$_2$(H$_2$O)](ClO$_4$)$_2$ cleaves SC DNA completely to generate both NC (95%) and LC (5%) forms. Interestingly, the dpq ligand is found not to cleave DNA under similar experimental conditions, and no significant cleavage is observed upon 365 nm irradiation when Cu(ClO$_4$)$_2$·6H$_2$O was used in place of **5**, revealing that mixed-ligand complex species are the active species (Figure S14A). When a singlet oxygen quencher, like sodium azide, was added to the reaction mixture, no inhibition of cleavage activity was noted, and when D$_2$O in which singlet oxygen has longer lifetime was used as solvent, no significant increase in cleavage is observed. These observations rule out the involvement of singlet oxygen (Scheme S1, type II) in the photoinduced DNA cleavage reactions. Further, the addition of the hydroxyl radical scavenger DMSO to the reaction mixture tends to inhibit the cleavage reaction, and only 35% cleavage (NC form) was observed, suggesting the involvement of hydroxyl radicals in the photocleavage reaction[47] (Figure S14B). We suggest that the photoexcited complex ([Cu^{II}(tdp)(dpq)]$^{+*}$) would follow a mechanistic pathway involving one- or two-electron reduction of the oxygen molecule to generate a hydroxyl radical (Scheme S1), rather than conversion of the oxygen molecule to singlet oxygen, which is generally observed in the photodynamic therapy (PDT) cycle. The highest Cu(II)/Cu(I) redox potential of **5** (cf. above, Table S6) suggests that the conversion of Cu(II) (d^9) to Cu(I) (d^{10}) by one-electron transfer in the excited state is facilitated, and the resulting Cu(I) center then activates dioxygen to form the hydroxyl radical[11c] (Scheme S1). These results indicate the important role of the partial intercaltion of the dpq ligand in **5** in conferring the highest DNA binding affinity. Obviously, the efficient photonuclease activity observed for **5** at lower concentration upon 365 nm irradiation for a short time is a significant result in the chemistry of copper-based nucleolytic agents.

Tryptophan Quenching Experiment. To investigate the interaction of the copper complexes with proteins, the tryptophan emission-quenching experiments were carried out using bovine serum albumin (BSA) in the presence of **1**−**5**. The emission intensity depends on the degree of exposure of the two tryptophan side chains,[48] 134 and 212, to polar solvent and also on its proximity to specific quenching groups, such as protonated carbonyl, protonated imidazole,

(44) Sreedhara, A.; Freed, J. D.; Cowan, J. A. *J. Am. Chem. Soc.* **2000**, *122*, 8814−8824.
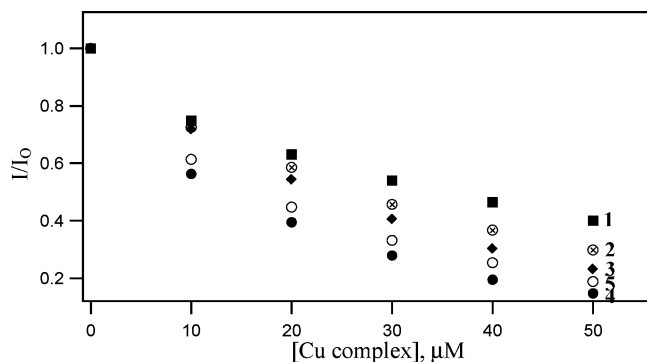(45) Liu, C.; Yu, S.; Li, D.; Liao, Z.; Sun, X.; Xu, H. *Inorg. Chem.* **2002**, *41*, 913−922.
(46) Kirin, S. K.; Happel, C. M.; Hrubanova, S.; Weyhermuller, T.; Klen, C.; Nolte, N. M. *Dalton Trans.* **2004**, 1201−1207.
(47) Collet, M.; Hoebeke, M.; Piette, J.; Lindqvist, L.; Van de Vorst, A. *J. Photochem. Photobiol. B.* **1996**, *35*, 221−231.
(48) Peters, T. *Adv. Protein Chem.* **1985**, *37*, 161−245.

Figure 6. Fluorescence quenching of BSA with and without **1**−**5** in phosphate buffer at pH 7.0. Excitation wavelength, 295 nm.

Table 2. In Vitro Cytotoxicity Assays for Complexes **1**−**5**, Cisplatin, and Mitomycin C against Human Cervical Epidermoid Carcinoma Cell Line (ME180)[a]

| | | IC$_{50}$ values[b] | |
		24 h	48 h
[Cu(tdp)]$^+$	**1**	81.36 ± 1.00	54.54 ± 1.00
[Cu(tdp)(bpy)]$^+$	**2**	31.01 ± 3.00	0.91 ± 0.05
[Cu(tdp)(phen)]$^+$	**3**	1.33 ± 0.01	0.72 ± 0.02
[Cu(tdp)(tmp)]$^+$	**4**	0.40 ± 0.01	0.29 ± 0.05
[Cu(tdp)(dpq)]$^+$	**5**	0.85 ± 0.07	0.70 ± 0.05
cisplatin		45.74 ± 1.00	1.89 ± 0.06
mitomycin C		53.65 ± 3.00	1.59 ± 0.03

[a] Data are mean ± SD of four replicates each. [b] IC$_{50}$ = concentration of drug required to inhibit growth of 50% of the cancer cells (in μM).

deprotonated ϵ-amino groups, and tyrosinate anions.[49a,b] The emission intensity of BSA, measured as described in the Experimental Section, is found to decrease in the presence of **1**−**5** because of possible changes in protein secondary structure leading to changes in tryptophan environment of BSA.[50] The ability of the complexes to quench the emission intensity of BSA follows the order **4** > **5** > **3** > **2** > **1**. Further, the higher slope for **4** in the plot of I/I_0 versus [complex] (Figure 6) reveals the stronger protein-binding ability of the tmp complex with enhanced hydrophobicity.

Anticancer Activity Studies. The anticancer activities of **1**−**5** against the ME180 human cervical epidermoid carcinoma cell line have been investigated in comparison with the widely used drugs (see introduction) cisplatin and mitomycin C under identical conditions by using MTT assay. Interestingly, as revealed by the the observed IC$_{50}$ values (Table 2), the tmp complex **4** exhibits potency approximately 100 and 6 times more than those of the two drugs for 24 and 48 h incubations, respectively. Complexes **3** and **5** exhibit potencies approximately 35 and 55 times, respectively, more than those of the two drugs for 24 h incubation, but they exhibit IC$_{50}$ values only two times lower than those of the two drugs for 48 h incubation. Complex **2** shows IC$_{50}$ values approximately 1.5 and 2 times lower than those of the two drugs for 24 and 48 h incubation respectively. On the other hand, Complex **1** shows IC$_{50}$ values higher than those of the two drugs for both 24 and 48 h incubations. This clearly

indicates that the cytotoxicities of the complexes are time dependent and vary with the mode and extent of their interactions with DNA and protein. It is evident that the hydrophobic forces of DNA interaction,[51] as exhibited by **4**, and the partial intercalative DNA interaction, as shown by **4** and **5**, lead to enhanced cytotoxicity.

To investigate the molecular mechanisms underlying the inhibitory effects of complexes on cell growth, we examined the different phases of the cell cycle by flow cytometry, which involves quantitative measurements of DNA content of cells. The ME180 cells were treated with IC$_{50}$ and IC$_{70}$ concentrations of **4** (0.29 and 0.45 μM) and **5** (0.70 and 1.4 μM), which show high activity in MTT assay, and then harvested after 24 h incubation. The PI-stained cells were assessed by flow cytometry with the FL2-A channel. The representative histograms shown in Figure 8 reveal that both complexes show a concentration dependent inhibition of ME180 cells. Compared to control cells, those exposed to **4** and **5** at their IC$_{50}$ concentrations are slightly arrested at the S[52a] and G$_2$/Mphases[52b,c] of the cell cycle and subsequently accumulated in the sub-G$_1$ phase at 24 h harvesting (Figure 7). Interestingly, the cells exposed to **4** and **5** at their IC$_{70}$ concentrations induced a marked decrease in the number of cells in phases G$_0$/G$_1$, S, and G$_2$/M and subsequently accumulated in the sub-G$_1$ phase (Figure 7), revealing the increase in apoptotic cell death.[52b,c,19a] This is supported by the typical fragmentation of apoptotic cells observed from microscopic analyses of cells treated with IC$_{50}$ values of **4** and **5** (see below). Thus it is obvious that **4** and **5** mediate the S and G$_2$/M phase arrest of the treated cells, which progress into apoptosis.

After the cells were treated with IC$_{50}$ concentrations of **1**−**5** for 24 and 48 h, they were analyzed for cytological changes such as chromatin fragmentation, binucleation, cytoplasmic vacuolation, nuclear swelling, cytoplasmic blebbing, and late apoptosis indication of dotlike chromatin condensation[53,3] with Hoechst 33258 staining. The results reveal that all the complexes bring about cytological changes (Figure S15) and that the cells are committed to a specific mode of cell death. All the complexes also display a necrotic and apoptosis mode of cell death. Further, the tmp complex **4** exhibits a percentage of apoptosis cell death higher than that of other complexes (Figure 8A). The data on the manual counting of cells with normal and abnormal nuclear features are shown in Figure 8B, and it is evident that the number of abnormal cells increases in a time-dependent manner.

All of the above observations clearly show that the dpq complex **5** exhibits DNA binding affinity and cleavage ability

(49) (a) Halfman, C. J.; Nishida, T. *Biochim. Biophys. Acta* **1971**, *243*, 284−293. (b) Halfman, C. J.; Nishida, T. *Biochim. Biophys. Acta* **1971**, *243*, 294−303.
(50) Quiming, N. S.; Vergel, R. B.; Nicolas, M. G.; Villanueva, J. A. *J. Health Sci.* **2005**, *51*, 8−15.

(51) Yan, K. Y.; Melchart, M.; Habtemariam, A.; Sadler, P. J. *Chem. Commun.* **2005**, 4764−4776.
(52) (a) Agarwal, M. K.; Hastak, K.; Jackson, M. W.; Breit, S. N.; Stark, G. R.; Agarwal, M. L. *Proc. Natl. Acad. Sci. U.S.A.* **2006**, *103*, 16278−16283 (b) Liu, T.; Xu, Z.; He, Q.; Chen, Y.; Yang, B.; Hu, Y. *Bioorg. Med. Chem. Lett.* **2007**, *17*, 278−281. (c) Lin, Y. H.; Yang, S. H.; Chien, C. M.; Hu, X. W.; Huang, Y. H.; Lu, C. M.; Chen, Y. L.; Lin, S. R. *Drug Dev. Res.* **2006**, *67*, 743−751.
(53) Kasibhatla, G. P. A. H.; Finucane, D.; Brunner, T.; Wetzel, E. B; Green, D. R. Protocol: Staining of suspension cells with Hoechst 33258 to detect apoptosis. *Cell:* A *laboratory manual Culture and Biochemical Analysis of Cells*; CSHL Press: USA, 1998; Vol. 1, pp.15.5.
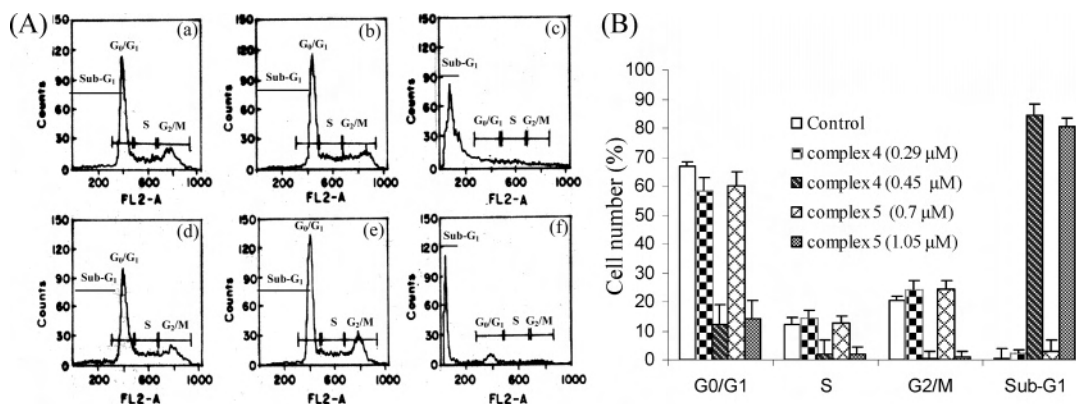
Figure 7. Effect of **4** and **5** on the distribution of ME180 cells in cell cycle populations. The cell cycle phase was determined by the cellular DNA content measured by flow cytometry of PI stained cells. G_1, S, and G_2/M denote the corresponding phases of the cell cycle. Sub-G_1 events correspond to cells or cell fragments with lower DNA content and are indicative of the apoptotic death of the cells. (A) Cell cycle distribution is shown as histograms. Untreated cells are used as control for **4** (a) and **5** (d) for 24 h harvesting time. Cells are treated with **4** at concentrations of 0.29 μM (b) and 0.45 μM (c) and with **5** at 0.70 μM (e) and 1.05 μM (f) for 24 h harvesting time. (B) The percentage of cells in each phase is indicated as a graph. Data are mean values obtained from three independent experiments and bars represent standard deviations.
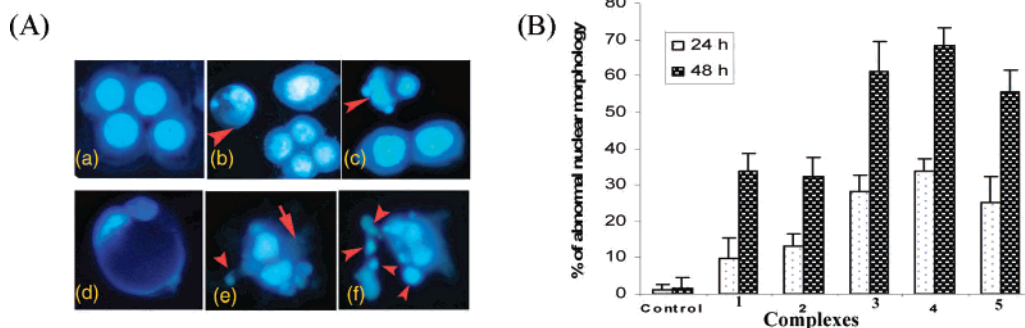
Figure 8. (A) Photomicrograph showing the features of Hoechst 33258 staining of ME180 cervical carcinoma cells. Cells were treated with **4** after 24 h seeding. The cells were stained with Hoechst 33258 fluorescent dye: (a) untreated cells (control), (b−f) treated with **4**; (b) cytoplasmic vacuolation and chromatin marginalization, (c) chromatin fragmentation, (d) cytoplasmic vacuolation and marginalization of nucleus, (e) cytoplasmic blebbing (arrow), apoptotic body formation (arrowhead) and binucleation, (f) late apoptosis indication of apoptotic bodies. Cells were treated with 0.29 μM of **4** after 24 h seeding. (B) Data showing counts of cells with normal and abnormal nuclear features. Abnormal cells increases in a time-dependent manner for **1**−**5**. Data are mean values obtained from two independent experiments and bars represent standard deviations.

higher than that of the other complexes. On the other hand, the tmp complex, which shows a weaker DNA binding and also lower DNA cleavage than **5**, is the only complex that causes a B to A conformational change on DNA and also exhibits a cytotoxicity higher than that of **5**. It is known that cisplatin exhibits a conformational deviation from B-type DNA upon platination and that the conformational changes induced by platinum complexes are directly related to the DNA-repair systems and cytotoxic profiles.[54] Similarly, the DNA conformational change caused by the tmp complex would be expected to interfere with the cellular function of DNA. Therefore, the higher cytotoxicity of the tmp complex would correlate with its ability to confer a conformational change on DNA and cleave it. It is also clear that a complex with a stronger DNA binding ability or a higher cleavage activity does not need to show a higher cytotoxicity. Further, the tmp complex is found to bind to the plasma protein BSA more strongly than the other complexes. Very recently,[55] the anticancer activity of certain ruthenium(III) complexes has been related to their ability to bind to proteins and cause

severe inhibition of some fundamental enzyme function. The protein-bound complexes are thought to be transported through biological fluids and eventually released at the cellular level to exhibit anticancer activity.[55] However, binding to plasma proteins might result in drastic modifications, or even loss, of the biological properties of the complex molecules. Therefore, we hypothesize that a drug, which binds to a protein or causes a conformational change on DNA, is likely to exhibit a higher cytotoxicity. Furthermore, the cell cycle arrest at S and G_2/M phases and subsequent accumulation in the sub-G_1 phase by the complexes **4** and **5** suggests that the complexes might inhibit the function of certain proteins, which play a key role in regulation of the cell cycle.[22] So, if the drug is to exhibit cytotoxicity by induction of apoptosis, it should target and inhibit some of the proteins involved in the cancer profile.[22] Thus it emerges from our present study that a conformational change on DNA, followed by DNA cleavage, and the ability to bind to proteins are the requisites for a drug to act as an anticancer agent. Further mechanistic investigations are needed to fully understand the detailed molecular mechanism of cytotoxicity and hence to verify our hypothesis.

(54) Zhao, Y.; He, W.; Shi, P.; Zhu, J.; Qiu, L.; Lin, L.; Guo, Z. *Dalton Trans.* **2006**, 2617−2619

(55) Messori, L.; Orioli, P.; Vullo, D.; Alessio, E.; Lengo, E. *Eur. J. Biochem.* **2000**, *267*, 1206−1213.

Conclusions

Simple and mixed-ligand copper(II) complexes of the tetradentate phenolate ligand H(tdp) with a series of diimine coligands have been isolated. The X-ray crystal structures of the 1:1 complex [Cu(tdp)(ClO$_4$)]·0.5H$_2$O and the mixed-ligand complex [Cu(tdp)(phen)](ClO$_4$)·CH$_3$OH contain Cu-(II) located in square-based geometries, which are retained in solution. The coordinated dpq and phen coligands of the mixed ligand complexes are involved in strong partial intercalation into the DNA base pairs in the minor groove. On the other hand, the tmp complex is involved in strong hydrophobic interaction with DNA through the four methyl groups on phen ring, which is relevant to its ability to confer the B to A conformational change on DNA.

All the complexes cleave supercoiled DNA in the presence of ascorbic acid as reducing agent and the phen and dpq complexes exhibit cleavage efficiencies higher than those of the other complexes. They cleave supercoiled DNA hydrolytically to nicked and linear forms in the absence of any external reagent. Further, interestingly, upon irradiation with 365 nm radiation, the strongly binding dpq complex effectively converts supercoiled DNA into nicked and linear forms through double-strand breaks.

It is noteworthy that among all the complexes the tmp complex, despite its lower DNA binding and cleavage activity than its dpq analogue, exhibits the highest anticancer activity against the human cervical epidermoid carcinoma (ME180) cell line. Its potency is also greater than those of cisplatin and mitomycin C, which are currently in clinical use for treating cervical cancer. The anticancer activity of this complex may originate from their ability to cause a conformational change on DNA and cleave it and also it ability to bind to the cellular proteins involved in inducing cancer. All the complexes bring about condensation and breakage of chromatin into clumps typical of apoptosis and also cause necrotic cell death. Thus, we have shown that the mixed-ligand tmp complex has the potential to be developed as an anticancer drug for treating cervical and possibly other forms of cancer.

Experimental Section

Reagents and Materials. Copper(II) perchlorate hexahydrate, 3,4,7,8-tetramethyl-1,10-phenanthroline (Aldrich), 1,10-phenanthroline, 2-(2-aminoethylamino)ethanol (Merck), salicylaldehyde (Loba chemie), calf thymus (CT) DNA (highly polymerized stored at 4 °C), superoxide dismutase (SOD), bovine serum albumin (BSA), catalase, (Sigma, stored at −20 °C), pBR322 supercoiled plasmid DNA, agarose, Lambda/Hind III, pUC18/Sau 3A I-pUC18/Taq I digest, T4 ligase, and ligation buffers (Genei, Bangalore, India) were used as received. Ultrapure MilliQ water (18.2 mΩ) was used in all experiments. The ligand dipyrido-[3,2-*d*:2′,3′-*f*]-quinoxaline (dpq) was prepared by the reported procedure.[56] The commercial solvents were distilled and then used for preparation of complexes.

Cell Culture. The ME180 human cervical cancer cell line was obtained from National Center for Cell Science (NCCS), Pune,

India. The cells were cultured in RPMI 1640 medium (Biochrom AG, Berlin, Germany), supplemented with 10% fetal bovine serum (Sigma), cisplatin (Getwell Pharmaceuticals, India), mitomycin C (Sigma,), and 100 U/mL penicillin and 100 μg/mL streptomycin as antibiotics (Himedia, Mumbai, India) in 96-well culture plates at 37 °C in a humidified atmosphere of 5% CO$_2$ in a CO$_2$ incubator (Heraeus, Hanau, Germany). All experiments were performed using cells from passage 15 or less.

Methods and Instrumentation. Microanalysis (C, H, and N) were carried out with a Vario EL elemental analyzer. An LCQ DECA XP electrospray mass spectrometer was employed for ESI-MS analysis. UV−vis spectroscopy was recorded on a Varian Cary 300 Bio UV−vis spectrophotometer using cuvettes of 1 cm path length. Electron paramagnetic resonance spectra of the mixed-ligand complexes were obtained on a Varian E 112 EPR spectrometer. The spectra were recorded for the solutions of the compound in DMF at liquid nitrogen temperature (LNT). DPPH was used as the field marker. Cerius 2 software was employed to obtain a energy-minimized structure of **4**. Emission intensity measurements were carried out using Jasco F 6500 spectrofluorometer. Circular dichroic spectra of DNA were obtained by using JASCO J-716 spectropolarimeter equipped with a peltier temperature control device. Viscosity measurements were carried out using Schott Gerate AVS 310 automated viscometer.

Solutions of DNA in the buffer 50 mM NaCl/5 mM Tris HCl in water gave a ratio of UV absorbance at 260 and 280 nm, A_{260}/A_{280}, of 1.9,[57] indicating that the DNA was sufficiently free of protein. Concentrated stock solutions of DNA (13.5 mM) were prepared in buffer and sonicated for 25 cycles, where each cycle consisted of 30 s with 1 min intervals. The concentration of DNA in nucleotide phosphate (NP) was determined by UV absorbance at 260 nm after 1:100 dilutions. The extinction coefficient, ϵ_{260}, was taken as 6600 M^{-1} cm^{-1}. Stock solutions were stored at 4 °C and used after no more than 4 days. Supercoiled plasmid pBR322 DNA was stored at −20 °C, and the concentration of DNA in base pairs was determined by UV absorbance at 260 nm after appropriate dilutions taking ϵ_{260} as 13 100 M^{-1} cm^{-1}. Concentrated stock solutions of metal complexes were prepared by dissolution of calculated amounts of metal complexes in a corresponding amount of solvent and were diluted suitably with the corresponding buffer to the required concentrations for all the experiments.

Preparation of H(tdp) and their Copper(II) Complexes. Synthesis of H(tdp). Salicylaldehyde (1.015 g, 10 mmol) in methanol (20 mL) was added dropwise to 2-(2-aminoethylamine)-ethanol (1.017 g, 10 mmol) in methanol (20 mL). The mixture was stirred for 2 h to get a bright yellow solution. The resulting solution was evaporated, and the yellow oily residue dried in vacuum (yield, 1.978 g, 95%).

Caution: During handling of the perchlorate salts of metal complexes with organic ligands care should be taken because of the possibility of explosion.

Synthesis of [Cu(tdp)(ClO$_4$)]·0.5H$_2$O (1). This complex was synthesized by adding a methanolic solution of the ligand (0.104 g, 0.5 mmol), which was deprotonated by using a solution of NaOH (0.5 mmol equivalent), to a solution of copper(II) perchlorate (0.1852 g, 0.5 mmol) in methanol solution and then stirring at 40 °C for 1 h. The resulting solution was filtered and then kept for slow evaporation at room temperature. The blue needle-shaped crystals suitable for X-ray diffraction were collected by suction filtration. Anal. Calcd for [Cu(tdp)(H$_2$O)(ClO$_4$)]: C, 34.84; H, 4.25; N, 7.39. Found: C, 34.74; H, 4.20; N, 7.29%.

(56) Collins, J. G.; Sleeman, A. D.; Aldrich, J. R.; Greguric I.; Hambly, T. W. *Inorg. Chem.* **1998**, *37*, 3133−3141.

(57) Merill, C.; Goldman, D.; Sedman, S. A.; Ebert, M. H. *Science* **1980**, *211*, 1437−1438.

Synthesis of [Cu(tdp)(bpy)]ClO₄ (2). This complex was prepared by addition of a methanolic solution of 2,2′-bipyridine (0.078 g, 0.5 mmol) and H(tdp) (0.104 g, 0.5 mmol), which was deprotonated by using a solution of NaOH (0.5 mM equivalent), to a solution of copper(II) perchlorate (0.185 g, 0.5 mmol) in methanol and then stirring at 40 °C for 1 h. The resulting solution was filtered and kept aside for slow evaporation at room temperature. The green crystalline solid separated out and was collected by suction filtration, washed with small amounts of methanol, and then dried in vacuum. Anal. Calcd for [Cu(tdp)(bpy)](ClO₄): C, 47.91; H, 4.40, N; 10.64. Found: C, 48.12; H, 4.47; N, 10.75%. ESI-MS: [Cu(tdp)(bpy)]⁺ displays a peak at m/z = 427.00, calcd = 426.98.

Synthesis of [Cu(tdp)(phen)]ClO₄·CH₃OH (3). This complex was isolated using the procedure adopted to obtain **2**. The green needle-shaped crystals suitable for X-ray diffraction were obtained by slow evaporation of a concentrated solution of the complex. Anal. Calcd for [Cu(tdp)(phen)](ClO₄): C, 49.49; H, 4.67; N, 9.62. Found: C, 49.15; H, 4.38; N, 9.42%. ESI-MS: [Cu(tdp)(phen)]⁺ displays a peak at m/z = 451.10, calcd = 451.00.

Synthesis of [Cu(tdp)(3,4,7,8-tmp)]ClO₄ (4). This complex was isolated using the procedure adopted to obtain **2**. The resulting solution was filtered and kept aside for slow evaporation at room temperature. The green crystalline solid that separated out was collected by suction filtration, washed with small amounts of methanol, and then dried in vacuum. Anal. Calcd for [Cu(tdp)-(3,4,7,8-tmp)](ClO₄): C, 53.46; H, 5.15; N, 9.24. Found: C, 53.55; H, 5.36; N, 9.42%. ESI-MS: [Cu(tdp)(tmp)]⁺ displays a peak at m/z = 507.10, calcd = 507.11 (Figure S16).

Synthesis of [Cu(tdp)(dpq)]ClO₄ (5). This complex was also prepared using the procedure adopted for the isolation of **2**. The resulting solution was filtered and kept aside for crystallization by slow evaporation at room temperature. The green crystalline solid that separated out was collected by suction filtration, washed with small amounts of methanol, and then dried in vacuum. Anal. Calcd for [Cu(tdp)(dpq)](ClO₄): C, 49.84; H, 3.85; N, 13.95. Found: C, 49.54; H, 3.56; N, 13.55%. ESI-MS: [Cu(tdp)(dpq)]⁺ displays a peak at m/z = 503.00, calcd = 503.04.

X-ray Crystallography. Suitable single crystals were obtained, and intensity data were collected at 153 K on a Stoe Mark II-Image Plate Diffraction System,[58] equipped with a two-circle goniometer, using MoKα graphite-monochromated radiation: image plate distance = 100 mm, ω rotation scans = 0−180° (at φ = 0°) and 0−20° (at φ = 90°), step Δφ = 1.5°, exposure = 2 min per image, 2θ range = 2.29−59.53°, $d_{min} - d_{max}$ = 17.779−0.716 Å. The structure was solved by direct methods using the program SHELXS-97.[59] The refinement and all further calculations were carried out using SHELXL-97.[60] Crystal refinement data are listed in Table 3. The H-atoms were included in calculated positions and treated as riding atoms using SHELXL default parameters. The non-H atoms were refined anisotropically, using weighted full-matrix least-squares on F^2. No absorption correction was applied. Graphical representations of the structure were made with POV-Ray, version 3.6.[61]

DNA Binding and Cleavage Experiments. Concentrated stock solutions of metal complexes were prepared by dissolution of metal

Table 3. Crystal Data and Structure Refinement for Complexes **1** and **3**

	1	3
empirical formula	CuC₁₁H₁₆ClN₂O₆.₅CuC₁₁-H₁₅N₂O₂ClO₄·0.5(H₂O)	CuC₂₄H₂₇ClN₄O₇
fw	379.25	582.50
cryst syst	monoclinic	hexagonal
space group	$P2_1/n$	$P6_1$
cryst size (mm)	0.27 × 0.27 × 0.23	0.40 × 0.35 × 0.35
λ (Å) (Mo Kα)	0.71073	0.71073
a (Å)	11.7700(10)	14.1018(5)
b (Å)	12.8750(8)	14.1018(5)
c (Å)	19.1517(15)	44.3740(19)
α (deg)	90	90
β (deg)	97.435(10)	90
γ (deg)	90	120
Z	8	12
density (calcd) (mg/m³)	1.746	1.519
θ for data collection (deg)	2.36−25.89	1.67−25.18
GOF on F^2	1.014	0.977
reflns collected	5394	8497
R1/wR2 [I > 2σ(I)]ᵃ	0.0456	0.0275
R1/wR2 (all data)ᵃ	0.0676	0.0320

ᵃ R1 = Σ||F$_o$| − |F$_c$||/Σ|F$_o$|; wR2 = {Σw[(F_o^2 − F_c^2)^2/Σw[(F_o^2)^2]}$^{1/2}$.

complexes in 10% DMF/5 mM Tris-HCl/50 mM NaCl buffer at pH 7.1 and dilution of the solution suitably with the corresponding buffer to required concentrations for all the experiments. For absorption and emission spectral experiments, the DNA solutions were pretreated with solutions of metal complexes to ensure no change in concentration of the metal complexes.

Absorption spectral titration experiments were performed by maintaining a constant concentration of the complex, varying the nucleic acid concentration, and adopting an experimental method described previously.[19c] From the observed spectral changes, the value of the intrinsic equilibrium DNA binding constant K_b was determined by regression analysis using an equation,[62,19c] which includes binding site size. Emission, circular dichroism, and viscosty studies on the DNA binding of the complexes were performed using the equipment and procedures described elsewhere.[19c]

Cyclic voltammetry (CV) and differential pulse voltammetry (DPV) were performed in a single-compartment cell with a three-electrode configuration on a EG&G PAR 273 potentiostat-gal-vanostat equipped with an PIV computer. The working electrode was a glassy carbon disk (0.384 cm²), and the reference electrode was a saturated calomel electrode. A platinum plate was used as the counterelectrode. The supporting electrolyte was 50 mM NaCl/5 mM Tris-HCl buffer at pH 7.1. Solutions were deoxygenated by purging with nitrogen gas for 15 min prior to measurements; during the measurements, a stream of N₂ gas was passed over the solution. All the experiments were carried out at 25.0 ± 0.2 °C, maintained by a Haake D8-G circulating bath.

The cleavage of DNA in the absence of activating agents was monitored using agarose gel electrophoresis. In reactions using supercoiled pBR322 plasmid DNA (form I, 40 μM) in 10% DMF/5 mM Tris-HCl/50 mM NaCl buffer at pH 7.1 was treated with metal complexes. The samples were incubated for 4 h at 37 °C. A loading buffer containing 25% bromophenol blue, 0.25% xylene cyanol, and 30% glycerol (3 μL) was added, and electrophoresis was performed at 60 V for 5 h in Tris-acetate-EDTA (TAE) buffer (40

(58) *X-Area*, version 1.17, and *X-RED32*, version 1.04; Stoe & Cie GmbH: Darmstadt, Germany, 2002.

(59) Sheldrick, G. M. *Acta Crystallogr.* **1990**, *A46*, 467.

(60) Sheldrick, G. *SHELXL-97*; Universität Göttingen: Göttingen, Germany, 1999.

(61) *Persistence of Vision Raytracer*, version 3.6; Persistence of Vision Pty. Ltd.: Scotland, 1997; http://www.povray.org/download/.

(62) Carter, M. T.; Rodriguez, M.; Bard, A. J. *J. Am. Chem. Soc.* **1989**, *111*, 8901−8911.

mM Tris base, 20 mM , acetic acid, 1 mM EDTA) using 1% agarose gel containing 1.0 μg/mL ethidium bromide. The gels were viewed in a Alpha Innotech Corporation Gel doc system and photographed using a CCD camera. Densitometric calculations were made using the AlphaEaseFC StandAlone software. The intensities of super-coiled DNA were corrected by a factor of 1.47 as a result of its lower staining capacity by ethidium bromide.[63] The cleavage efficiency was measured by determination of the ability of the complex to convert the supercoiled DNA (SC) to nicked circular form (NC) and linear form (LC).

The decrease in the intensities of form I (SC) or the increase in the intensities of form II (NC) was then plotted against catalyst concentrations, and these were fitted well with a single-exponential decay curve (pseudo-first-order kinetics) by the use of known equations.[43] For anaerobic experiments, deoxygenated water and anaerobic stock solutions were prepared. To identify the reactive oxygen species (ROS) involved in the cleavage reaction, the radical scavengers such as hydroxyl radical (DMSO, 10%), singlet oxygen (NaN$_3$, 100 μM), superoxide (SOD, 10 unit), and H$_2$O$_2$ (catalase, 0.1 unit) were introduced. Ligation reactions were performed as follows: after incubation of pBR322 plasmid DNA with metal complex for 4 h at 37 °C, the cleaved (form II) was recovered by precipitation with 3.0 M NaOAc and 95% ethanol.[64] The plasmid was then incubated for 24 h at 16 °C with 10 U T4 ligase in the buffer provided by the supplier. In control experiments, the T4 ligase reactions were carried out also on Lambda/Hind III, pUC18/Sau 3A I-pUC18/Taq I digest. The reaction products were resolved on 1% agarose gel in TAE buffer.

The DNA cleavage with added reductant was monitored as in the case of cleavage experiment without added reductant using agarose gel electrophoresis. Reactions using supercoiled pBR322 plasmid DNA (SC, 40 μM, in base pair) in 10% DMF/5 mM Tris-HCl/50 mM NaCl buffer at pH 7.1 were treated with the metal complex (30 μM) and ascorbic acid (10 μM), followed by dilution with the Tris-HCl buffer to a total volume of 20 μL. The samples were incubated for 0.5 h at 37 °C, and the gel electrophoresis was performed as described above.

For photocleavage studies, the reactions were carried out under illuminated conditions at 365 nm (12 W) monochromatic light source. In each experiment, the sample was incubated for 1 h at 37 °C and analyzed for the photocleaved products using gel electro-phoresis as discussed above. Reactions using supercoiled pBR322 plasmid DNA (SC, 40 μM, in base pair) in 10% DMF/5 mM Tris-HCl/50 mM NaCl buffer at pH 7.1 was treated with the metal complex (25 μM), followed by dilution with the Tris-HCl buffer to a total volume of 20 μL. The inhibition reactions for the photonuclease studies were carried out at 365 nm using reagents (NaN$_3$, 100 μM; DMSO, 10%) prior to the addition of the complex. For the D$_2$O experiment, the same solvent was used for dilution to 18 μL.

Tryptophan Fluorescence Quenching. Quenching of the tryptophan residues of BSA[50] was done using complexes **1**−**5** as quenchers. To solutions of BSA in phosphate buffer at pH 7.0, increments of the quencher were added, and the emission signals at 344 nm (excitation wavelength at 295 nm) were recorded after each addition of the quencher. The I/I_0 versus [complex] plot was constructed using the corrected fluorescence data taking into account the effect of dilution.

Cell Viability Assay. MTT assay was carried out as described previously.[65] Complexes **1**−**5**, in a concentration of 0.05−100 μM, dissolved in DMSO (Sigma-Aldrich, St. Louis, MO), were added to the wells 24 h after they were seeded with 5×10^3 cells per well in 200 μL of fresh culture medium. DMSO was used as the vehicle control. After 24 and 48 h, 20 μL of MTT solution [5 mg/mL in phosphate-buffered saline (PBS)] was added to each well, and the plates were wrapped with aluminum foil and incubated for 4 h at 37 °C. The purple formazan product was dissolved by addition of 100 μL of 100% DMSO to each well. The absorbance was monitored at 570 nm (measurement) and 630 nm (reference) using a 96 well-plate reader (Bio-Rad, Hercules, CA,). The stock solutions of the metal complexes were prepared in DMSO, and in all the experiments, the percentage of DMSO was maintained in the range of 0.1−1%. DMSO by itself was found to be nontoxic to the cells up to a 1% concentration. Data were collected for four replicates each and were used to calculate the mean. The percentage inhibition was calculated, from this data, using the formula:

$$\frac{\text{mean OD of untreated cells (control)} - \text{mean OD of treated cells}}{\text{mean OD of untreated cells (control)}} \times 100$$

The IC$_{50}$ values were calculated using Table Curve 2D, version 5.01

Analysis of Cell Cycle Progression. Cells were seeded in a 25 cm^2 flask at a density of 1×10^6 cells/flask. After 24 h, CKBM with a final concentration of IC$_{50}$ or IC$_{70}$ was added to the respective flasks and incubated for 24 and 48 h. Cells were trypsinized, harvested, and fixed in 5 mL of 80% cold ethanol in test tubes and incubated at 4 °C for 15 min. After incubation, the cells were centrifuged at 1500 rpm for 5 min, and the cell pellets were resuspended in 500 μL of propidium iodine (10 μg/mL) containing 300 μg/mL RNase (Sigma, MO). Then cells were incubated on ice for 30 min and filtered with 53 μm nylon mesh. Cell cycle distribution was analyzed by using FACScan (Becton-Dickinson, San Jose, CA) with 15 mw, 488 nm argon ion laser. PI signals were collected using 585/42 band-pass filter. The data were acquired and analyzed with Cell Quest software.

Hoechst 33258 Staining. Cell pathology was detected by staining the nuclear chromatin of trypsinized cells (4.0×10^4/mL) with 1 μL of Hoechst 33258 (1 mg/mL, aqueous) for 10 min at 37 °C. Staining of suspension cells with Hoechst 33258 was performed to detect apoptosis.[53] A drop of cell suspension was placed on a glass slide and a cover-slip was laid over to reduce light diffraction. At random, 300 cells were observed in a fluorescent microscope (Carl Zeiss, Jena, Germany) fitted with a 377−355 nm filter observed at ×400 magnification, and the percentage of cells reflecting pathological changes were calculated. Data were collected for four replicates and were used to calculate the mean and the standard deviation.

(63) Bernadou, J.; Pratviel, G.; Bennis, F.; Girardet M.; Meunier, B. *Biochemistry* **1989**, *28*, 7268−7275.

(64) Maniatis, D.; Fritsch E. F.; Sambrook, J. *Molecular Clonong: A Laboratory Manual*; Cold Spring Harbor Laboratory Press: Plainview, NY, 1998; p 149.

(65) Blagosklonny, M.; El-Diery, W. S. *Int. J. Cancer* **1996**, *67*, 386−392.

Supporting Information Available: Tables of S1−S9, Scheme S1, and Figures of S1−S16. This material is available free of charge via the Internet at http://pubs.acs.org.

IC700755P